Submitted to Journal of Physics
and Chemistry of Solids

UCRL-19675
Preprint

LIBRARY AND
DOCUMENTS SECTION

# DESCRIPTION OF THE HYDROGEN-METAL INTERACTION BY A MORSE POTENTIAL FUNCTION

D. R. Olander

October 1970

AEC Contract No. W-7405-eng-48

TWO-WEEK LOAN COPY

*This is a Library Circulating Copy which may be borrowed for two weeks. For a personal retention copy, call Tech. Info. Division, Ext. 5545*

LAWRENCE RADIATION LABORATORY
UNIVERSITY of CALIFORNIA BERKELEY

UCRL-19675

## DISCLAIMER

This document was prepared as an account of work sponsored by the United States Government. While this document is believed to contain correct information, neither the United States Government nor any agency thereof, nor the Regents of the University of California, nor any of their employees, makes any warranty, express or implied, or assumes any legal responsibility for the accuracy, completeness, or usefulness of any information, apparatus, product, or process disclosed, or represents that its use would not infringe privately owned rights. Reference herein to any specific commercial product, process, or service by its trade name, trademark, manufacturer, or otherwise, does not necessarily constitute or imply its endorsement, recommendation, or favoring by the United States Government or any agency thereof, or the Regents of the University of California. The views and opinions of authors expressed herein do not necessarily state or reflect those of the United States Government or any agency thereof or the Regents of the University of California.

# DESCRIPTION OF THE HYDROGEN-METAL INTERACTION BY A MORSE POTENTIAL FUNCTION

by D.R. Olander

Inorganic Materials Research Division of
the Lawrence Radiation Laboratory and
the Department of Nuclear Engineering
University of California
Berkeley, California 94720

## Abstract

The interaction between hydrogen atoms adsorbed on the surface or dissolved in the interstices of a metal and the atoms of the host crystal is represented by a pairwise additive Morse potential function. This interaction is summed over all metal atoms surrounding the hydrogen atom. Interactions between hydrogen atoms are not considered. The three force constants of the potential function are determined from three experimental values of the hydrogen-metal system: the heat of solution, the heat of adsorption and the activation energy for bulk migration. Relaxation of the metal lattice surrounding the dissolved hydrogen and reconstruction of the surface metal atoms next to the adsorbed hydrogen are considered in the calculation. The potentials so determined are long range- metal atoms many lattice constants distant from the hydrogen atom contribute to the binding and the metal atoms closest to a dissolved hydrogen atom are repulsive. Four metals are treated: BCC iron and tantalum, and FCC nickel and copper. For each metal, two surface planes are investigated. Although both tetrahedral and octahedral interstitial sites were tested as solution sites, only occupancy of octahedral sites satisfied the interaction energies upon which the calculation is based. Knowledge of the potential function permits other characteristics of the hydrogen-metal interaction, such as the activation energy for surface migration and the vibration frequency of dissolved hydrogen, to be computed. Agreement of these calculated properties with experimental data is satisfactory, but not quantitative. The extreme sensitivity to crystal structure (BCC or FCC) and the assumption that the nature of the binding of surface hydrogen is the same as that of bulk hydrogen limit the utility of the pairwise model to that of an interpolation scheme - as a means of utilizing known characteristics of the hydrogen-metal system to estimate parameters not experimentally available.

# I. INTRODUCTION

Characteristics of the interaction of hydrogen with the regular lattice of a metal are investigated analytically. The metal-hydrogen interaction is represented by summation of a central pairwise potential function over all the metal atoms surrounding a hydrogen atom in or on the lattice. The pairwise potential is assumed to be the Morse function. This function is applicable to the interaction of the two hydrogen atoms of the hydrogen molecule (1) and it has also been applied to the binding properties of the metal lattice (2). The Morse potential (restricted to nearest neighbor interactions) has also been utilized to predict the equation of state of metals (3). This study seeks to determine whether the mixed case of the metal-hydrogen system can be satisfactorily analyzed by the same type of potential function. An investigation similar in many aspects to the one undertaken here has been reported by Goodman (4), who used a Lennard-Jones 6-12 interatomic potential to investigate the binding of various adsorbed species on tungsten and nickel. Johnson et al (5) used a cubic potential to investigate the properties of iron and vanadium. While Goodman's study was concerned solely with surface interactions, and the calculations of Johnson et al dealt only with bulk properties, the present work examines both surface and bulk interactions of hydrogen and the host metal.

The calculation does not purport to be a fundamental representation of the nature of the hydrogen-metal bond. In fact, the notion of central pairwise additivity may not

be applicable to such systems (4); Tamm and Schmidt (6), for example, have been able to explain the structure of hydrogen adsorbed on the (100) plane of tungsten on the basis of nearest neighbor bonds between the hydrogen atom and the d electrons of the metal. The present calculation should be viewed as an interpolation scheme - as a method of utilizing three relatively easily obtainable characteristics of the binding in a metal-hydrogen system to deduce other features of the system which are not experimentally available. In order to perform such a function, it is necessary to be able to describe the energy of a hydrogen atom at various locations in or on the crystal. Only the pairwise interaction model with an adjustable-parameter interaction potential provides a sufficiently complete calculational framework for this purpose.

Three experimental parameters of the hydrogen-metal system are employed to deduce the three force constants in the Morse potential function:

$$\phi(r) = D\left\{\exp\left[-2\,\frac{m}{r_e}\,(r-r_e)\right] - 2\exp\left[-\,\frac{m}{r_e}\,(r-r_e)\right]\right\} \qquad (1)$$

where $\phi(r)$ is the potential energy between the two atoms separated by a distance r and $r_e$, m, and D are the force constants ($r_e$ is the equilibrium separation of the two atoms and D is the energy of the interaction at the equilibrium separation distance). Knowledge of the interatomic potential function permits calculation of properties of the hydrogen-metal system other than the three used to determine the force constants. The validity of the method is assessed by

comparing the predicted properties to available measurements. Auxiliary features of the interaction, such as relaxation of the host atoms around a dissolved hydrogen atom and reconstruction of the surface as a consequence of hydrogen adsorption, cannot at this time be verified by comparison with experiment.

Several additional assumptions concerning the behavior of hydrogen in the metal lattice are:

(1) Hydrogen is dilute in the metal; H - H interactions either in the interior or on the surface of the metal are neglected. In concentrated solutions, this interaction must be considered (7,8). The dissolution equilibrium is assumed to follow Sievert's law, which implies hydrogen in atomic form in the bulk.

(2) The dissolved hydrogen behaves as a three dimensional Einstein oscillator in the interstitial site of the BCC or FCC lattice in which it is located. This model has been discussed by Ebisuzaki and O'Keefe (9) and applied to the solution and diffusion of hydrogen in nickel by Ebisuzaki, Kass, and O'Keefe (10). The assumption of an Einstein oscillator appears to be satisfactory for FCC metals, but is on somewhat tenuous grounds for BCC metals (9). Nevertheless, it is assumed here to apply to hydrogen dissolved in both types of cubic structures.

(3) Dissolved hydrogen may reside in either the tetrahedral or octahedral interstices of the cubic lattices. No assumption concerning this point is made; the calculations are performed for both types of equilibrium sites.

(4) Binding of hydrogen on the surface is of the same type as that in the bulk.

(5) The measured heats of adsorption refer to polycrystalline material with unidentified surface structure. In order to perform the calculations, the exposed surface plane must be specified. The (100) and (110) planes of the BCC lattice and the (110) and (111) planes of the FCC lattice have been considered here. In each case, the heat of adsorption is assumed to apply to the surface face under consideration.

(6) The diffusional jump is assumed to be from one equilibrium site to another via the other type of interstitial site (e.g., octahedral-tetrahedral-octahedral). The difference between the energy of the hydrogen atom in octahedral and tetrahedral sites is the activation energy of diffusion.

There is some support for this idea from other studies of migration of interstitial impurities in BCC lattices (5,11). As shown in Figure 1, the straight line path between octahedral sites in the BCC lattice passes through the tetrahedral interstitial site at the midpoint.

However, the octahedral-tetrahedral-octahedral path in the FCC lattice is not a straight line, as shown in Fig. 1 (the tetrahedral site shown is at the (1/4,1/4,1/4) position). Nevertheless, the hydrogen-metal distance in the tetrahedral site ($\sqrt{3}$ a/4, where a is the lattice constant) is larger than the hydrogen-metal distance at the midpoint of a straight line jump between two octahedral sites ($a/\sqrt{8}$), so that the path shown in Fig. 1 is not unreasonable. The diffusion of hydrogen in nickel has been shown to be in satisfactory agreement with octahedral-tetrahedral-jump (10).

The following aspects of the hydrogen-metal interaction are considered:

(1) the zero point energy of the dissolved hydrogen.

(2) relaxation of the host lattice about the dissolved and adsorbed hydrogen atoms.

(3) the difference between the separation of the surface layer of metal atoms and the adjacent layer, and the bulk planar separation.

Four metals are considered: BCC α-iron and tantalum and FCC nickel and copper. The parameters of the Morse function for the metal-metal interactions have been taken from the calculations of Girifalco and Weizer (2). The complete set of input parameters for the calculations are shown in Table 1. The lattice constant at room temperature is shown in the second column. The force constants for the metal-metal interaction are in columns 3-5. The sixth

column contains the calculated relaxation of the surface layer obtained from the force constants shown in the preceding columns (12). The quantity P is the difference between the calculated position of the surface plane and the position the surface would have if the bulk interplanar spacing were maintained to the surface.

The three parameters of the hydrogen-metal interaction which were used in the calculations are shown in the last three columns. $\chi_a$ represents the binding energy of atomic hydrogen on the surface, $\chi_s$ represents the heat of solution of atomic hydrogen and $\chi_d$ is the activation energy for bulk diffusion. A survey of the available literature indicates general accord (to within one or two kcal/mole) on all of these values except for the activation energy for diffusion of hydrogen in tantalum. The NMR measurements of Pedersen et al (13) on hydrides with hydrogen content exceeding $TaH_{0.1}$ yield a value of 1.6 kcal/mole. The classic permeation experiments reviewed by Chandler and Walter (14) yield larger values. Although the activation energy from permeation experiments may be falsified by the existence of a rate-controlling surface step, the activation energy in concentrated H-Ta solutions may reflect H-H interactions. On balance, we have selected the 14.0 kcal/mole result of Klyachko (15), since it was obtained by experiments more closely reflecting the high temperature, dilute solutions to which the present calculations apply.

Parameters of the hydrogen-metal system used to check the reasonableness of the calculations were:

(A) Surface diffusion activation energy

(B) Effect of surface plane on the hydrogen binding energy

(C) The vibrational partition function for motion of the adsorbed hydrogen perpendicular to the surface

(D) Pre-exponential factor of the solubility (entropy of solution)

(E) The internal vibration frequencies of hydrogen in nickel and copper

(F) The effect of the lattice type on the solubility parameters (the solubility of hydrogen in both BCC $\alpha$-Fe and FCC $\gamma$-Fe has been measured)

# II. ANALYSIS

## A. Heat of Solution

The ground state is the perfect metal lattice and free hydrogen atoms at rest. The dissolved state is the hydrogen atom in its lowest vibrational state at the center of an octahedral or tetrahedral interstice. The nearest and next nearest metal atom neighbors are allowed to relax. The energy released upon adding a hydrogen atom to the solid is given by:

$$\chi_s = -V_s - \Delta E_s - \frac{3}{2} h\nu_s \qquad (2)$$

where $V_s$ is the potential energy of the hydrogen atom in the relaxed solution site. $\Delta E_s$ is the increase in the potential energy of the metal atoms surrounding the hydrogen atom due to relaxation. $\nu_s$ is the vibrational frequency of the hydrogen atom in the equilibrium solution site. The last term is the zero point energy of the dissolved hydrogen atom.

## B. Binding Energy of Adsorbed Hydrogen Atoms

The adsorbed hydrogen atom is assumed to be in its ground state with respect to vibration perpendicular to the surface on the surface site which maximizes the binding energy. The adsorption sites were taken to be those determined by Goodman (4) for each surface plane considered. The positions of the adjacent metal atoms and the distance of the hydrogen atom above the surface are adjusted to

maximize the binding energy. The energy released on placing a free hydrogen atom on the surface is:

$$\chi_a = -V_a(z_{eq}) - \Delta E_a - \frac{1}{2} h\nu_a \qquad (3)$$

where $V_a(z_{eq})$ is the potential energy of the hydrogen atom at its equilibrium adsorption distance $z_{eq}$ and $\Delta E_a$ is the energy required to reconstruct the surface. The third term on the right is the zero point energy for vibration of the hydrogen atom perpendicular to the surface. $\nu_a$ is the frequency of this mode of vibration. The lateral binding is assumed weak and the zero point energy of these vibrational modes is assumed to be negligible.

C. Activation Energy for Bulk Diffusion

The activation energy for diffusion is:

$$\chi_d = (V_d - V_s) - (\Delta E_s - \Delta E_d) \qquad (4)$$

where $V_d$ is the potential energy of the hydrogen atom in the interstitial position chosen as the migration barrier and $\Delta E_d$ is the increase in lattice potential energy due to relaxation of the metal atoms about the hydrogen atom in this site. Transition state theory suggests that the right hand side of Eq(4) should contain another term reflecting the zero point energies in the equilibrium and activated

states. Ebusizaki et al (10) have shown that this additional term is of the form:

$$-kT\left[\frac{3}{2}\left(\frac{h\nu_s}{kT}\right)\coth\left(\frac{h\nu_s}{2kT}\right) - \left(\frac{h\nu^\dagger}{kT}\right)\coth\left(\frac{h\nu^\dagger}{2kT}\right) - 1\right]$$

where $\nu^\dagger$ is the frequency of the two vibrational modes perpendicular to the migration path in the activated state. If $\nu_s = \nu^\dagger$, the bracketed term in Eq(5) is always positive. However, for hydrogen in nickel, Ebusizaki et al (10) have measured $\nu^\dagger/\nu_s = 1.7$. In this case, the bracketed term is negative and Eq(5) adds ∿1 kcal/mole to the right hand side of Eq(4). This correction is approximately 10% of the energy of migration. Since the correction term of Eq(5) may be either positive or negative and since it appears to be small compared to the remaining terms in Eq(4), it has been neglected here. The treatment of diffusional migration energy is thus similar to that used by Burton and Jura (16) and Huntington (17).

D. Potential Energy of Hydrogen in the Bulk Metal

The potential energies $V_s$, $V_d$ and $V_a$ are obtained by summing the interaction potential between the hydrogen atom and a metal atom over all metal atoms in the lattice. To simplify this procedure, the infinite sum is approximated by a finite sum over ∿40 individual metal atoms closest to the hydrogen atom and an integral representing the interaction with the metal atoms at larger distances. The sums are accomplished by dividing the nearby metal atoms

into spherical shells in which the metal atoms are equidistant from the central hydrogen atom.

The characteristics of these shells for the two interstitial sites in the two cubic lattices considered are shown in Table 2. The cut-off distance is chosen midway between the last shell of atoms included in the sum and the next shell further out. Beyond the cut-off distance, the central hydrogen is considered to interact with a continuum of atom density equal to that of the solid. In seeking the maximum energy configuration, shells 1 and 2 are permitted to relax radially by factors of $q_1$ and $q_2$ respectively. The potential energy of the hydrogen atom in the interstitial site is:

$$V = \sum_{i=1}^{N} n_i \phi(q_i r_i^o) + 4\pi\gamma \int_{r_c}^{\infty} r^2 \phi(r) dr \qquad (6)$$

In this formula, V refers either to $V_s$ of Eq(2) or $V_d$ of Eq(4). N is the number of shells over which the sum is carried (N=6 for BCC and 3 or 4 for FCC), and $n_i$ is the number of atoms in shell i. $r_i^o$ is the hydrogen-metal distance of an atom in unrelaxed shell i, shown in the last column of Table 2. $q_i$ is zero for i>2. The function $\phi$ is the Morse potential of Eq(1). The last term in Eq(6) represents the contribution of the continuum atom distribution at distances greater than the cut-off $r_c$ to the total interaction energy. $\gamma$ is the number of atoms in the unit cell of the metal (2 for BCC, 4 for FCC).

E. Potential Energy of Hydrogen on the Surface

The potential energy of a hydrogen atom at a distance

z over a particular surface site is determined by a sum over hemispherical shells of equidistant metal atoms plus a continuum contribution:

$$V_a(z) = \sum_{i=1}^{N} n_i \phi(r_i) + 2\pi\gamma \int_{r_c}^{\infty} r^2 dr \int_0 \phi[(z^2 + r^2 + 2rz\mu)^{1/2}] d\mu \qquad (7)$$

The origin of the spherical coordinate system used in the integration is directly beneath the adsorbed atom on the surface plane which would exist in the absence of separation of the outer most layer of metal atoms. z is the distance of the adatom above this plane, r is the radial distance from the origin to a point in the continuum and $\mu$ is the cosine of the polar angle referred to the axis perpendicular to the surface and passing through the origin. The number of shells over which the sum is carried is chosen to give a cut-off radius $r_c$ as close as possible to that used in the computation of the interaction energy in the bulk. In general, the first term on the right of Eq(7) includes one half as many metal atoms ($\sim$20) as the corresponding internal sum. Because of the lower degree of symmetry of the lattice below a hydrogen atom on the surface compared to a centrally placed hydrogen atom in an interstitial site, a larger number of shells are required. For the BCC(100) and (110) surfaces and the FCC(110) surface, the shells were structured in accord with Figs. 1 and 2 of Goodman's paper (4). There are two potential adsorption sites in the FCC(111) face. The adatom

nestles in the crevice formed by three surface metal atoms. However, there may or may not be a metal atom directly beneath the adsorbed atom (these two situations are depected as the B and C sites in Fig. 27a of ref. 18). Our calculations indicate only a few percent difference in the binding energy on these two sites with the "C" site (no metal atom directly below the adsorbed hydrogen) slightly

more tightly bound. This site was taken as the adsorption site.

The foregoing considerations refer to the perfect crystal surface. To these calculations were added the separation of the entire outer layer of metal atoms from the bulk and the relaxation of the metal atoms close to the adsorbed hydrogen atom. The configurations of the surfaces for the four cases considered is shown in Fig. 2. On the BCC(100) surface, the metal atom directly beneath the adatom is permitted to move vertically and the nearest neighbor metal atoms on the surface may relax radially and vertically. On the BCC(110) surface, only radial and vertical relaxation of the nearest neighbor atoms on the surface is allowed. Relaxation on the FCC(110) surface is equivalent to that on the BCC(100) face. The three surface atoms closest to the adsorbed hydrogen atom on the FCC(111) adsorption site relax radially and vertically. The three atoms in the next layer may relax in a radial direction only. These relatively restricted degrees of relaxations were designed to keep the calculations tractable yet still provide a qualitative estimate of the significance of surface reconstruction.

The shell distances $r_i$ in Eq(7) are functions of the hydrogen adsorption distance z. If the atoms considered are subject to relaxation or if the shell contains surface metal atoms, $r_i$ also depends on the outer layer spacing P,

and the relaxation parameters $s_1$, $s_2$, and $s_3$.

F. Lattice Relaxation Energies

The energy required for lattice relaxation about a hydrogen atom in the solution site or in the activated site ($\Delta E_s$ or $\Delta E_d$) is a function of the relaxation the nearest and next-nearest neighbor shells surrounding the hydrogen atom ($q_1$ and $q_2$) and the Morse potential force constants for the metal-metal interaction. Following Burton and Jura (19), only radial relaxation is allowed. The interaction energy between the N shells in which discrete atom positions are considered and between the discrete atom shells and the continuum is:

$$E_s(q_1,q_2) = \sum_{i=1,\neq 2}^{N} E_{1i}(q_1) + E_{12}(q_1,q_2) + E_{1c}(q_1) + \sum_{i=2}^{N} E_{2i}(q_2) + E_{2c}(q_2) \qquad (8)$$

Interactions between atoms whose positions do not change during the relaxation process are not included in Eq(8) since these cancel out in computing $\Delta E_s$.

$E_{ji}$ is the interaction energy between atoms in shells i and j and is given by:

$$E_{ji} = \sum \phi(r_{ij}) \ , \qquad (j = 1,2)$$

where the summation runs over all bonds between atoms in shell i and shell j. For the self-energy of a single shell containing $n_i$ atoms, there are $\frac{1}{2} n_i(n_i-1)$ bonds. Between two different shells, there are $n_i n_j$ bonds. $r_{ij}$ is the distance between a pair of atoms in the i and j shells, and is a function of the relaxation parameters $q_1$ and/or $q_2$. The Morse potential function in Eq(9) utilizes the force constants appropriate to the metal under consideration (Table 1).

$E_{1c}$ and $E_{2c}$ denote the interaction energy between shells 1 and 2 and the continuum beginning at the cut-off distance $r_c$. The energy of interaction between shell j containing $n_j$ atoms at a distance $q_j r_j^o$ from the hydrogen atom and the continuum is:

$$E_{jc}(q_j) = 2\pi\gamma n_j \int_{r_c}^{\infty} r^2 dr^2 \int_{-1}^{1} \phi[\{(q_j r_j^o)^2 + r^2 - 2r(q_j r_j^o)\mu\}^{1/2}] d\mu \ , \qquad (j = 1,2) \tag{10}$$

where $\phi$ is again the metal-metal potential function, $r_j^o$ and $r_c$ are taken from the last column of Table 2 and $\mu$ is the cosine of the polar angle in the spherical coordinate system with origin at the hydrogen atom.

The suitability of this method for determining relaxation energies was tested by computing the energy of sublimination of the perfect metal lattice. In this test,

the shells were constructed around a central metal atom and the sublimation energy computed by:

$$\Delta E_{sub} = -\frac{1}{2}\left\{\sum n_i \phi(r_i) + 4\pi\gamma \int_{r_c}^{\infty} r^2 \phi(r) dr\right\} \tag{11}$$

where $n_i$ and $r_i$ are the number of atoms in the ith shell and the distance of this shell from the central atom respectively. These parameters were taken from the compilation of ref. 20. The cut-off distance was taken mid-way between the Nth and the (N+1)th shells. For N=8, the computed sublimation energy was within a fraction of a percent of the value used by Girifalco and Wiezer (2) to determine the force constants shown in Table 1. For N=4, the number of discrete atoms considered in the lattice sum was ∿40, as in the hydrogen-metal calculations. In this case, the computed sublimation energy was within 3-4% of the correct value. This magnitude of error introduced by the continuum approximation to the lattice sum is considered acceptable for the calculations here.

Thus, for specified values of the first and second shell relaxation factors, the increase in the energy of the metal lattice surrounding the hydrogen atom is given by:

$$\Delta E_s = E_s(q_1, q_2) - E_s(1,1) \tag{12}$$

The energy required to reconstruct the surface, $\Delta E_a$, is computed in an entirely analogous fashion, with the surface relaxation parameters $s_1$, $s_2$, and $s_3$ replacing $q_1$ and $q_2$.

## G. Vibration Frequencies

The vibration frequency of the interstitial hydrogen atom is determined by averaging out the angular dependence of the interaction energy between the hydrogen atom slightly displaced from its equilibrium position and the metal atoms in the N surrounding shells. This procedure forces the potential well to be spherically symmetric. The angle-averaged potential between a hydrogen atom at a distance $\rho$ from its equilibrium position and one of the atoms of shell i at a distance $q_i r_i^o$ from the center of the cell is given by:

$$\overline{\phi}_i(\rho) = \frac{1}{2}\int_{-1}^{1} \phi[\{\rho^2 + (q_i r_i^o)^2 - 2\rho(q_i r_i^o)\mu\}^{1/2}]d\mu \qquad (13)$$

The total potential energy of the hydrogen atom in the off-center position is:

$$V(\rho) = \sum_{i=1}^{N} n_i \overline{\phi}(\rho) + 2\pi\gamma \int_{r_c}^{\infty} r^2 dr^2 \int_{-1}^{1} \phi[(\rho^2 + r^2 - 2\rho r\mu)^{1/2}]d\mu \qquad (14)$$

In Eqs(13) and (14), $\phi$ refers to the hydrogen-metal interaction potential.

The energies computed by Eq(14) fit the parabolic form:

$$V(\rho) - V(0) = \frac{1}{2}\kappa_s \rho^2 \qquad (15)$$

to within a few percent for displacements up to 1/5 of a lattice parameter. The vibration frequency was determined

from the value of $\kappa_s$ obtained by fitting $V(\rho)$ according to Eq(15):

$$\nu_s = \frac{1}{2\pi}\left(\frac{\kappa_s}{m}\right)^{1/2} \tag{16}$$

where m is the mass of the hydrogen atom.

The frequency of perpendicular vibration of an adsorbed hydrogen atom, $\nu_a$, was determined by fitting $V_a(z)$ of Eq(7) to a parabola about the equilibrium adsorption distance $z_{eq}$.

H. Determination of the Force Constants

The problem contains the following unknowns:

(a) The force constants m, $r_e$, and D of the hydrogen-metal Morse potential function.

(b) The bulk relaxation parameters $q_{1s}$ and $q_{2s}$ for the solution site and $q_{1d}$ and $q_{2d}$ for the activated site.

(c) The equilibrium adsorption distance $z_{eq}$.

(d) The surface relaxation parameters $s_1$, $s_2$, and $s_3$.

Sufficient equations to determine these parameters are obtained by using Eqs(2) -(4) and the requirement that at equilibrium, the interaction energies must be a maximum. Applying the latter condition to the heat of solution expressed by Eq(2):

$$\frac{\partial V_s}{\partial q_{js}} + \frac{\partial \Delta E_s}{\partial q_{js}} = 0 , \qquad (j = 1,2) \tag{17}$$

Since the zero point energy term in Eq(2) is small compared to the other terms, its variation with the relaxation parameters is neglected.

For the activated site the equilibrium condition is:

$$\frac{\partial V_d}{\partial q_{jd}} + \frac{\partial \Delta E_d}{\partial q_{jd}} = 0 , \qquad (j = 1,2) \tag{18}$$

The surface binding energy is maximized with respect to the adsorption distance:

$$\frac{\partial V_a}{\partial z} = 0 \qquad \text{at } z = z_{eq} \tag{19}$$

In obtaining this equation from Eq(3) the effect of the relaxation energy of the lattice, $\Delta E_a$, and the zero point energy, $\frac{1}{2} h\nu_a$, both of which are small compared to $V_a(z)$, have been neglected.

The surface binding energy is maximized with respect to the surface relaxation parameters:

$$\frac{\partial V_a}{\partial s_i} + \frac{\partial \Delta E_a}{\partial s_i} = 0 , \qquad (i = 1,2,3) \tag{20}$$

Eqs(2) - (4) and (17) - (20) constitute a set of 11 algebraic equations to be solved for 11 unknowns. The solution was effected numerically on a digital computer. Each of the metals in Table 1 was investigated. In each case, solution was attempted for the octahedral solution site-tetrahedral activated site and the reverse situation.

For a specified metal and a particular solution site, two adsorption planes were considered. These planes are shown in Fig. 2 for the two lattice types.

## III. CALCULATED FORCE CONSTANTS AND RELAXATIONS

Solutions were obtainable only for the combination of an octahedral solution site and a tetrahedral activated site. In no case did the *a priori* choice of the tetrahedral solution site yield a set of force constants which could reproduce the input interaction energies of Table 1. The results of the computations for the octahedral solution site are shown in Table 3.

Except for tantalum, solutions were obtained for both of the low index surface planes considered as adsorption sites in each of the cubic structures. The choice of adsorption plane had a minor effect on the computed force constants.

Again excepting tantalum, the hydrogen-metal interaction potentials are longer range $[(r_e)_{H-M} > (r_e)_{M-M}]$ and broader $(m_{M-H} < m_{M-M})$ than the host metal interaction parameters (compare Tables 1 and 3). Fig. 3 illustrates the Fe-H Morse potential and the Fe-Fe potential taken from reference 2, as well as the positions of the first six shells of equidistant atoms surrounding the central atom. It can be seen that the first two shells of the Fe-H interaction are repulsive rather than attractive. Qualitatively, the reason for this behavior lies in the relative magnitude of the heats of solution and adsorption and the assumption that the metal-hydrogen forces in the bulk and on the surface are of the same type. Table 1 shows that in all cases the heat of solution is smaller than the hydrogen binding energy on the surface.

Yet in the bulk, the hydrogen atom is surrounded by an infinite sea of metal atoms, while on the surface only a semi-infinite volume of metal atoms are available to bind the hydrogen. The only way that surface binding can be stronger than bulk binding when there are only half as many atoms with which to interact is for a substantial part of the bulk interaction to be non-binding (i.e. repulsive). Although the hydrogen-metal distances in an interstitial site are fixed by the lattice geometry (excluding relaxation for the moment), the surface hydrogen atom need only move away from the surface to escape the repulsive interaction characteristic of the interatomic distances separating the dissolved hydrogen atom and the first two interior shells. In the Fe-H case, the repulsive component of the first two shells is just cancelled by the attraction of the next four shells, and the entire heat of solution is due to interaction of the hydrogen atom with the continuum of metal atoms beyond the cut-off distance.

Since the pairwise model used here results in interaction forces of quite long range, it is easy to see why hydrogen in the octahedral site is more stable than in the tetrahedral site. In the FCC lattice, the nearest neighbors to a hydrogen atom in a tetrahedral site are significantly closer to the hydrogen atom than in the octahedral configuration. Consequently, the first shells are even more strongly repulsive in the tetrahedral case than in the octahedral case. The situation is not so clear cut in the BCC lattice. In the unrelaxed configuration, the two metal atoms

constituting the first shell of the BCC octahedral interstice are closer to the central hydrogen atom than are the four metal atoms of the first shell of the tetrahedral site. However, the relaxation of the octahedral first shell is considerably greater than that of the tetrahedral first shell (since in there are only two atoms in the former and four in the latter). The net result is that in the BCC lattice, the first two shells of the octahedral site are somewhat less repulsive in nature than the first two shells of the tetrahedral site. Consequently, the binding energy is greater in the octahedral site.

Although Table 3 indicates that the computed force constants are relatively insensitive to the adsorption face, the effect of lattice type is very marked. The heats of solution and adsorption of the hydrogen-iron and hydrogen-nickel systems are very close, which suggests similar H-metal interaction potentials (the difference between the bulk migration energies is in the direction expected from the geometrical considerations discussed in the preceding paragraph). Yet Table 3 shows a distinct difference in the shapes of the Fe-H and Ni-H potential functions. The latter is even longer range and broader than the Fe-H potential. Because of this difference, and because of the closer packing of the FCC lattice compared to the BCC structure, the hydrogen atom in the nickel interstitial site interacts with many more metal atoms than in iron. Consequently, to give roughly the same binding energies, the bond energy, D, is appreciably less

for the Ni-H interaction than the Fe-H interaction. This exaggerated influence of the crystal structure (which is even more dramatically illustrated by the computed difference in solubility of hydrogen in $\alpha$ and $\gamma$ iron) is a defect in the pairwise model applied to such systems. From the previous arguments, this effect of structure would probably remain if other forms of the potential function were used.

It is a general feature of the model that the larger the bulk migration energy, the shorter range are the computed potentials. This is especially striking in comparing the Fe-H and Ta-H results. In the latter instance the equilibrium separation, $r_e$, is even smaller than that of the Ta-Ta potential function. However, because $\chi_a > \chi_s$ in in the Ta-H system, the first shell surrounding the hydrogen atom in the octahedral site is still repulsive. In the FCC lattice, the computed potentials are quite long range despite migration energies of $\sim$9 kcal/mole. This is a reflection of the much smaller H-metal distance in the tetrahedral site than in the octahedral site for the FCC of lattice compared to the BCC lattice. Shorter range Ni-H or Cu-H forces would have required even larger migration energies.

Table 3 shows that the relaxation of the metal atoms in the octahedral site of the BCC lattice is large; the first shell is displaced outward by $\sim$20% and the second shell contracts by 3% in the case of tantalum and expands by 2% in the case of iron. The relatively short range

potential in the Ta-H system is similar to the potential employed for the Fe-C system by Johnson et al (5), and the relaxations of the octahedral sites surrounding the impurity atom are also similar in magnitude. In addition, the relaxations of the first two shells of the octahedral site surrounding a dissolved carbon atom were found to be radially symmetric. In the Fe-C, Fe-H and Ta-H systems, the spherical configuration adjacent to the impurity atom is deformed into a prolate spheroid. Relaxation of the tetrahedral site in the present case is different from that in the carbon-iron analysis of Johnson et al (5). Although the maximum first shell tetrahedral relaxation of 11% is of the same order of magnitude as that calculated for the hydrogen solute considered in this study, the Fe-C tetrahedral site relaxation was not of the purely radial displacement type.

Because of the longer range and greater width of the computed potentials in the FCC systems considered here compared to the BCC lattice, the forces on the nearest neighbors atoms are not as great in the former. Hence, the relaxation of the interstitial sites in the FCC cases are less than in the BCC systems.

Table 3 shows that the disruption of the surface by the adsorbed hydrogen is small. In all cases the surface atoms which are nearest neighbors to the adsorbed hydrogen atom are displaced radially outward and downward in the final configuration. When three degrees of relaxation are allowed, the displacements do not exceed 2% of a lattice constant.

The larger displacements in the BCC(110) case are probably due to the fact that only two degrees of relaxation were allowed. The largest energy of surface relaxation is ∿3 kcal/mole which is small compared to the adatom binding energy. Similarly, the zero point energy for adatom vibration perpendicular to the surface is small. The equilibrium adsorption distances are between $\frac{1}{2}$ and $\frac{3}{4}$ of a lattice constant. Although not shown in Table 3, sizeable variation of the first layer separation distance (P of Table 1) produced only minor changes in the computed force constants.

The zero point energy of vibration of the dissolved hydrogen constitutes ∿15% of the heat of solution for the BCC metals and about 7% for the FCC metals.

# IV. COMPARISON WITH OTHER MEASUREMENTS

## A. Activation Energy for Surface Migration

The measurement of interest here is the ratio of the activation energy for surface migration to the binding energy in the adsorption site, which is denoted by Q. This parameter has been determined by Gomer and co workers to be 0.22 for hydrogen on tungsten (21) and 0.11 for hydrogen on nickel (22). In calculating the surface migration energy from the potential functions, the migration sites were taken to be those utilized by Goodman (4); for the FCC(111) surface, the migration site was assumed to be the location midway over the line joining two surface metal atoms.

Because of the similarity of tantalum and tungsten and their very nearly equal hydrogen binding energies, the experimental H-W results may be compared to the H-Ta calculations. Only the (110) surface yielded a solution for the potential function in the H-Ta system. The Q value computed for this face of tantalum was 0.16, compared to the 0.22 experimental value for hydrogen on tungsten.

Although experimental measurements of Q are not available for the surface diffusion of hydrogen on iron, the calculations were performed for both the (100) and (110) faces. The corresponding Q values were 0.16 and 0.06 respectively. As expected, binding is much more uniform on the close packed (110) plane than on the rougher (100) plane, and the surface migration energy is lower on the former

(20). These Q values for iron are similar in magnitude and direction to those calculated by Goodman (4) for hydrogen on tungsten using a 6-12 potential function.

For FCC nickel, the calculated Q value is 0.04 for the (100) face. This is significantly smaller than the experimental value of 0.11. However, the experimental observation of a lower value of Q for an FCC crystal face compared to a BCC surface is reflected in the calculations. The calculated binding energy on the migration site for the FCC(111) face was negative by ∿1 kcal/mole compared to the binding energy on the selected adsorption site. This means that the sites chosen as adsorption and migration positions should have been reversed. The energy difference between these two sites, however, is very slight (∿2% of the binding energy). The FCC(111) surface is a good illustration of Ehrlich's description of a metal surface as one over which the hydrogen atom interacts continuously, with minor perturbations in the binding energy at adsorption sites (23).

The Q values for hydrogen on copper were essentially equal to those for hydrogen on nickel.

B. Effect of Surface Plane on the Hydrogen Binding Energy

It appears to be a general rule that binding of adatoms is weaker on close packed planes than on rougher ones (21,24). In each of the cubic crystal systems investigated here, one of the two surfaces was the close packed plane (the (110) plane in the BCC structure and the (111) plane in the FCC lattice).

In the BCC system, the difference between the binding

energy of hydrogen on the (100) and (110) planes was 6% of the binding energy for iron and 40% for tantalum. On the BCC(100) surface, the adatom can adjust its position above the surface to maximize the interaction energy with the four equidistant surface nearest neighbor metal atoms (see Fig. 2). On the BCC(110) surface, however, the four surface metal atoms adjacent to the adsorbed atom are not equidistant from the latter. Consequently, the hydrogen-metal interaction cannot be optimized as efficiently as for the (100) surface, and binding is weaker on the (110) plane. As expected, the shorter range and narrower H-Ta interatomic potential accentuates this structural effect.

The effect of surface orientation is much less pronounced for the FCC system than for the BCC structure. The calculated hydrogen-metal forces are longer range and the substrate metal is more densely packed in the former. These two factors decrease the importance of the immediate environment of the adatom; a larger portion of the surface binding energy is due to the more distant atoms. The difference in the hydrogen binding energy on the (110) and (111) planes of the FCC lattice is 3% of the binding energy for both nickel and copper.

C. Vibration Perpendicular to the Surface

Assuming that the adsorbed hydrogen atom behaves as a two-dimensional ideal gas, the rate constant for atom evaporation can be determined from the principle of detailed balancing (23). The rate constant so calculated is inversely

proportional to the partition function for adatom vibration perpendicular to the surface, which is:

$$j_{\perp} = \left[1 - \exp\left(-\frac{h\nu_a}{kT}\right)\right]^{-1} \tag{21}$$

Hickmott (25) has measured the rate of desorption of hydrogen atoms from tungsten. The experimental rate constant suggests a partition function $j_{\perp} \sim 1.3$. Taking tantalum as a stand-in for tungsten and using the vibration frequency $\nu_a$ computed by the method described in Sec. II-G, a value of $j_{\perp}$ of 1.2 is computed for a temperature of 1000°K. Both experiment and calculation suggest that on the refractory metals, the adsorbed hydrogen is very nearly in its ground vibrational state.

D. Pre-exponential Factor in the Solubility

The Einstein oscillator model used to describe the behavior of hydrogen in an interstitial site in the metal forms the basis of the Fowler-Smithells solubility expression (26):

$$\frac{c}{\sqrt{p_2}} = S_o \exp\left(\frac{\chi_s - \frac{1}{2} D}{kT}\right) \tag{22}$$

where c is the concentration of dissolved hydrogen in atoms/cm$^3$, $p_2$ is the pressure of molecular hydrogen gas in dynes/cm$^2$, and D is the dissociation energy of molecular hydrogen

(103 kcal/mole).

The pre-exponential factor $S_0$ may be written as:

$$S_0 = \frac{\omega_s n_s j_s}{2^{3/4}(kTj_{2rot})^{1/2}\lambda_1^{3/2}}\left(\frac{\lambda_1}{a}\right)^3 \tag{23}$$

where $j_{2rot}$ is the rotational partition function for molecular hydrogen gas, $\omega_s$ is the number of spin states available to the electron brought into the metal with the hydrogen atom and $n_s$ is the number of solution sites per unit cell (12 and 6 for the BCC tetrahedral and octahedral sites, respectively; 8 and 4 for the FCC tetrahedral and octahedral sites, respectively). $\lambda_1$ is the thermal wave length of the hydrogen atom:

$$\lambda_1 = \frac{h}{\sqrt{2\pi mkT}} \tag{24}$$

at T = 1000°k, $\lambda_1$ = 0.55Å. $j_s$ is the partition function of the dissolved hydrogen. For the Einstein oscillator model,

$$j_s = \left[1 - \exp\left(-\frac{h\nu_s}{kT}\right)\right]^{-3} \tag{25}$$

The internal vibration frequency, $\nu_s$, is obtained by the methods of Sec. II-G. The temperature dependent quantities in Eq(23) were evaluated at 1000°K, which represents an average temperature of the solubility measurements. Table 4 compares the measured and calculated values of the pre-exponential factor $S_0$. The calculated values are all lower

than the experimental ones. The discrepancies are probably due to the neglect of the excess entropy of mixing, which arises from the change in vibration frequency of the metal atoms adjacent to the dissolved hydrogen and the stored energy in the elastic continuum resulting from relaxation. Huntington et al (26) have calculated an excess entropy of 0.8k for a copper interstitial in copper; this provides a factor of ∿2 increase in the pre-exponential factor of the solubility. Inclusion of the excess entropy in the hydrogen solubility expression of Eq(23) undoubtedly would have driven the calculated values closer to the experimental ones.

E. Internal Vibration Frequencies

Comparison of the solubilities of hydrogen and deuterium in the same metal permits the internal vibration frequency of hydrogen in the metal to be determined (9). Such experiments have been performed on nickel and copper; they yield values of the vibrational energy level spacing $h\nu_s$ of 2.7 and 3.1 kcal/mole for hydrogen in nickel and copper respectively (9). The calculations here yield 2.3 and 2.2 kcal/mole respectively.

The calculated vibrational level spacings in the BCC metals are significantly larger, being 3.9 and 7.2 kcal/mole for hydrogen in iron and tantalum, respectively. There are no directly comparable experimental values. Sakamoto (27) has measured the vibration frequency of hydrogen in the

tetrahedral site of the face-centered tetragonal lattice of $TaH_{0.7}$ by neutron diffraction. His result corresponds to an energy level spacing of 3.3 kcal/mole.

F. Hydrogen Solubility in γ-Iron

The parameters of the hydrogen-iron Morse potential shown in Table 3 were determined from the BCC structure of α-iron. This potential function was utilized to calculate the heat of solution of hydrogen in FCC γ-iron. The octahedral site was assumed to be the solution site and an estimated value of the lattice constant of γ-iron at 300°K was utilized in order to keep the calculation on the same basis as that for α-iron. The calculated heat of solution is 56 kcal/mole. Experimentally, the heat of solution of hydrogen in γ-iron is essentially equal to the 45 kcal/mole value for α-iron (9). The pairwise model calculation fails rather clearly on this point. This failure is more significant than, say, the five-fold difference between calculated and experimental solubilities in copper shown in Table 4. The prediction of the heat of solution in γ-iron involves only the potential function itself and is not obscured by unknown effects such as the excess entropy of solution which may account for some of the discrepancies in the figures in Table 4.

In the case of the disparity between the H-Fe and H-Ni potential functions discussed in Sec. III, essentially similar binding energies yielded different potential functions. Here, the situation is one in which the same potential function

yields significantly different binding energies for two different crystal structures of the same metal. The reason is again structural and can be seen by examining the contributions to $\chi_s$ according to Eqs(2) and (6). The zero point energies are approximately equal for the two modifications of iron. When the same potential function that gives the host lattice relaxation energy of 34 kcal/mole in α-iron is applied to γ-iron, the relaxation energy is found to be 24 kcal/mole. As in the case of the BCC form, the sum in Eq(6) for FCC iron contributes ∿0 to the binding energy and the continuum contributions are approximately the same for the two phases. Thus for the estimated γ-iron lattice constant of 3.595Å at 300°K, the major part of the difference in hydrogen binding in the BCC and FCC lattices is due to the difference in the relaxation energies of the metal atoms around the dissolved hydrogen in the two cases.

The heat of solution computed from Eqs(2) and (6) for a specified potential function is the difference between energy terms comparable in magnitude to the heat of solution itself. Such a calculation is quite sensitive to small errors in the computation of each term and to the input parameters. For example, a 1% error in the estimated lattice constant of γ-iron produces a 2 kcal/mole change in the heat of solution.

The same sensitivity (and failure to obtain quantitative agreement) was observed by Johnson et al (5) when their Fe-C

potential function determined from the properties of carbon in α-iron was applied to predict the interaction energy of orthorhombic $Fe_3C$.

## V. NEAREST NEIGHBOR INTERACTIONS ONLY

The results of Tamm and Schmidt (6) suggest that adsorbed hydrogen bonds only to adjacent metal atoms (on the (100) face of tungsten at least). To simulate this type of bonding (retaining the Morse potential function), the entire set of calculations were rerun with only nearest neighbor interactions permitted. In the bulk this amounted to restricting interactions to the first two shells of the BCC octahedral site and the first shell of the other three interstices (see Table 2). On the surface, the hydrogen atom was permitted to interact only with the metal atoms shown in the sketches of Fig. 2 (except for the FCC(111) face, where the three atoms in the second layer were replaced by a single atom directly beneath the adatom - the B site was used instead of the C site). All other aspects of the calculation were the same as in the case that hydrogen was permitted to interact with all surrounding atoms.

No solutions were found for the set of input hydrogen-metal interaction energies shown in Table 1. Bulk migration energies much larger than those shown in the last column of Table 1 would have been required to produce reasonable potential functions. The nearest-neighbor-only restraint renders the computation completely dependent upon the structure and distances of the metal atoms adjacent to the hydrogen atom. This extreme structural sensitivity is

greatly mitigated by allowing longer range interactions, which was done in the original computations. The intermediate restraint employed by Johnson et al (5) of forcing the potential to go to zero at some point between the second and third shells was not attempted.

# VI. CONCLUSIONS

The computational method of utilizing three parameters of the hydrogen-metal interaction to infer other characteristics of the system using the pairwise additive Morse potential function as a vehicle provides satisfactory qualitative results. It is an adequate interpolation technique for estimating some hard-to-measure features of the hydrogen-metal system. "Fine structure", such as the relative magnitude of the internal vibration frequencies in copper and nickel discussed in Sec. IV-E, is not faithfully reproduced. The method is excessively sensitive to the structure of the bulk crystal, but not to the adsorption face to which the surface binding energy is assumed to refer.

The method is applicable only to dilute solutions. The pairing of hydrogen atoms in the metal, which has recently been shown to be important even at quite small hydrogen concentrations (28), is ignored. The actual state of dissolved hydrogen is not considered. Although hydrogen is believed to be ionized in metals (9), this fact affects the present calculations only in the rather inconsequential choice of the electron spin factor in Eq(23). However, the long range of the potentials computed in this study (binding is due in large part to interaction of hydrogen with metal atoms many lattice constants distant)

TABLE 2

SHELLS FOR COMPUTING LATTICE SUMS FOR DISSOLVED HYDROGEN

| Interstitial Site | Shell Number | Number of atoms in shell | 4 times the H-metal distance in units of the lattice constant (unrelaxed)* |
|---|---|---|---|
| BCC-octahedral | 1 | 2 | $\sqrt{4}$ |
| | 2 | 4 | $\sqrt{8}$ |
| | 3 | 8 | $\sqrt{20}$ |
| | 4 | 8 | $\sqrt{24}$ |
| | 5 | 10 | $\sqrt{36}$ |
| | 6 | 8 | $\sqrt{40}$ |
| | cut-off | --- | $\sqrt{46}$ |
| BCC-tetrahedral | 1 | 4 | $\sqrt{5}$ |
| | 2 | 4 | $\sqrt{13}$ |
| | 3 | 8 | $\sqrt{21}$ |
| | 4 | 12 | $\sqrt{29}$ |
| | 5 | 4 | $\sqrt{37}$ |
| | 6 | 12 | $\sqrt{45}$ |
| | cut-off | --- | $\sqrt{49}$ |
| FCC-octahedral | 1 | 6 | $\sqrt{4}$ |
| | 2 | 8 | $\sqrt{12}$ |
| | 3 | 24 | $\sqrt{20}$ |
| | cut-off | --- | $\sqrt{28}$ |
| FCC-tetrahedral | 1 | 4 | $\sqrt{3}$ |
| | 2 | 12 | $\sqrt{11}$ |
| | 3 | 12 | $\sqrt{19}$ |
| | 4 | 16 | $\sqrt{27}$ |
| | cut-off | --- | $\sqrt{31}$ |

*The ratio of the distance of closest approach to the lattice constant is $\sqrt{3}/2$ for the BCC lattice and $1/\sqrt{2}$ for the FCC lattice.

TABLE 3

RESULTS - OCTAHEDRAL SOLUTION SITE (all energies in kcal/mole)

| Metal | H-Metal Force Constants | | | Internal Relaxation | | | | | | Surface Relaxation | | | | | | |
|---|---|---|---|---|---|---|---|---|---|---|---|---|---|---|---|---|
| | | | | Octahedral Site | | | Tetrahedral Site | | | | | | | | | |
| | $r_e/a$ | m | D | $q_1$ | $q_2$ | $\Delta E_s$ | $q_1$ | $q_2$ | $\Delta E_d$ | $s_1$ | $s_2$ | $s_3$ | $\Delta E_a$ | $\frac{3}{2}h\nu_s$ | $\frac{1}{2}h\nu_a$ | $z_{eq}/a$ |
| Fe(100) | 1.12 | 2.96 | 4.6 | 1.199 | 1.019 | 33.8 | 1.118 | 0.999 | 34.3 | -.002 | .008 | -.020 | 1.4 | 6.0 | 1.1 | 0.58 |
| Fe(110) | 1.17 | 2.93 | 4.3 | 1.206 | 1.022 | 37.1 | 1.124 | 0.999 | 37.8 | .015 | -.087 | --- | 2.7 | 5.8 | 1.2 | 0.73 |
| Ta(110) | 0.75 | 3.94 | 17.0 | 1.191 | 0.971 | 48.9 | 1.087 | 0.990 | 44.0 | .014 | -.044 | --- | 2.8 | 10.9 | 1.9 | 0.45 |
| Ni(110) | 1.31 | 2.74 | 1.4 | 1.037 | 1.005 | 7.8 | 1.058 | 1.007 | 9.9 | .005 | .005 | -.019 | 0.8 | 3.4 | 0.8 | 0.64 |
| Ni(111) | 1.35 | 2.75 | 1.4 | 1.040 | 1.006 | 8.9 | 1.061 | 1.008 | 10.9 | .000 | -.004 | .000 | 0.2 | 3.4 | 0.8 | 0.80 |
| Cu(110) | 1.26 | 2.76 | 1.4 | 1.042 | 1.005 | 7.9 | 1.066 | 1.007 | 10.0 | .006 | .005 | -.021 | 0.8 | 3.2 | 0.7 | 0.62 |
| Cu(111) | 1.29 | 2.76 | 1.4 | 1.045 | 1.006 | 9.1 | 1.070 | 1.008 | 11.4 | .000 | -.005 | .000 | 0.2 | 3.3 | 0.8 | 0.78 |

TABLE 4

PRE-EXPONENTIAL FACTORS IN THE SOLUBILITY OF HYDROGEN IN METALS

| METAL | $S_0 \times 10^{-16}$, atoms/cm$^3$/(dynes/cm$^2$)$^{\frac{1}{2}}$ CALCULATED[a] | EXPERIMENTAL[b] |
|---|---|---|
| Fe | 11 | 20 ± 2 |
| Ta | 4.8 | 4.9 ± 0.3 |
| Ni | 8 | 30 ± 3 |
| Cu | 8 | 40 ± 3 |

[a]These are average values for the two surface planes considered for each metal. The spin term in Eq(23) was assumed to be unity.

[b]taken from the compilation of ref. 9 and J.D. Fast, Interaction of Metals and Gases, Vol. I, Academic Press (1965). The tantalum average also includes the measurement of ref. 15. The error indicates the spread among the sources used in obtaining the averages.

## LITERATURE CITED


1. E.A. Moelwyn-Hughes, Physical Chemistry, 2nd Ed., MacMillan (1961).

2. L.A. Girifalco and V.G. Weizer, Phys. Rev. 114, 687 (1959).

3. D.J. Pastine, J. Appl. Phys. 35, 3407 (1964); R.J. Naumann, NASA TN D-5892 (1970).

4. F.O. Goodman, Phys. Rev. 164, 1113 (1967).

5. R.A. Johnson, G.J. Dienes and A.C. Damask, Acta. Metal. 12, 1215 (1964).

6. P.W. Tamm and L.D. Schmidt, J. Chem. Phys. 51, 5352 (1969).

7. M. Hoch, Trans. AIME, 230, 138 (1964).

8. R.V. Bucur and M. Crisan, J. Phys. Chem. Solids, 28, 995 (1967).

9. Y. Ebisuzaki and M. O'Keefe, Prog. in Sol. State Chem. 4, 187 (1967).

10. Y. Ebisuzaki, W.J. Kass, and M. O'Keefe, J. Chem. Phys. 46, 1373 (1967).

11. D.N. Beshers, in Diffusion in Body-Centered Cubic Metals, Amer. Soc. for Metals, p. 149 (1965).

12. J.J. Burton and G. Jura, J. Phys. Chem. 71, 1937 (1967).

13. B. Pedersen, J. Krogdahl and O.E. Stokkeland, J. Chem. Phys. 42, 72 (1965).

14. W.T. Chandler and R.J. Walter, in Refractory Metal Alloys, I. Machlin, R.T. Gegeley and E.D. Weisert, eds., p. 197, Plenum Press (1968).

15. I.A. Klyachko, L.L. kunin, S.P. Fedorov, and I.N. Larionov, Akademiia Nauk SSSR. Komissiia po Analiticheskoi Khimii. Trudy 10, 49 (1960). Also translated as UCRL-Trans-1375.

16. J.J. Burton and G. Jura, J. Phys. Chem. Solids, 28, 705 (1967).

17. H.B. Huntington, Phys. Rev. 91, 1092 (1953).

18. C. Kittel, Introduction to Solid State Physics, 3rd ed., p. 29, Wiley (1967).

19. J.J. Burton and G. Jura, J. Phys. Chem. Solids, 27, 961 (1966).

20. J. O. Hirschfelder, C.F. Curtiss, and R.B. Bird, Molecular Theory of Gases and Liquids, p. 1037, Wiley (1964).

21. R. Gomer, R. Wortman, and R. Lundy, J. Chem. Phys. 26, 1147 (1957).

22. R. Wortman, R. Gomer, and R. Lundy, J. Chem. Phys. 27, 1099 (1957).

23. G. Ehrlich, Trans. of the 8th Vac. Symp., Pergammon, p. 126 (1962).

24. G. Ehrlich, Trans. Farad. Soc., 41, 7 (1966).

25. T.W. Hickmott, J. Chem. Phys. 32, 810 (1960).

26. H.B. Huntington, G.A. Shirn, and E.S. Wajda, Phys. Rev., 99, 1085 (1955).

27. M. Sakamoto, J. Phys. Soc. Japan 19, 1862 (1964).

28. A.D. McQuillan, J. Chem. Phys. 53 (1970).

# FIGURE CAPTIONS

1. Octahedral-octahedral migration paths via the tetrahedral site
2. Surface configurations after adsorption (distances in units of the lattice constant)
3. The iron-iron interaction potential (2) and the hydrogen-iron interaction potential. Positions of shells surrounding central atom are marked. The shell positions in the Fe-H system are for the octahedral site. Shells 1 and 2 of the Fe-H system are in the relaxed configuration.

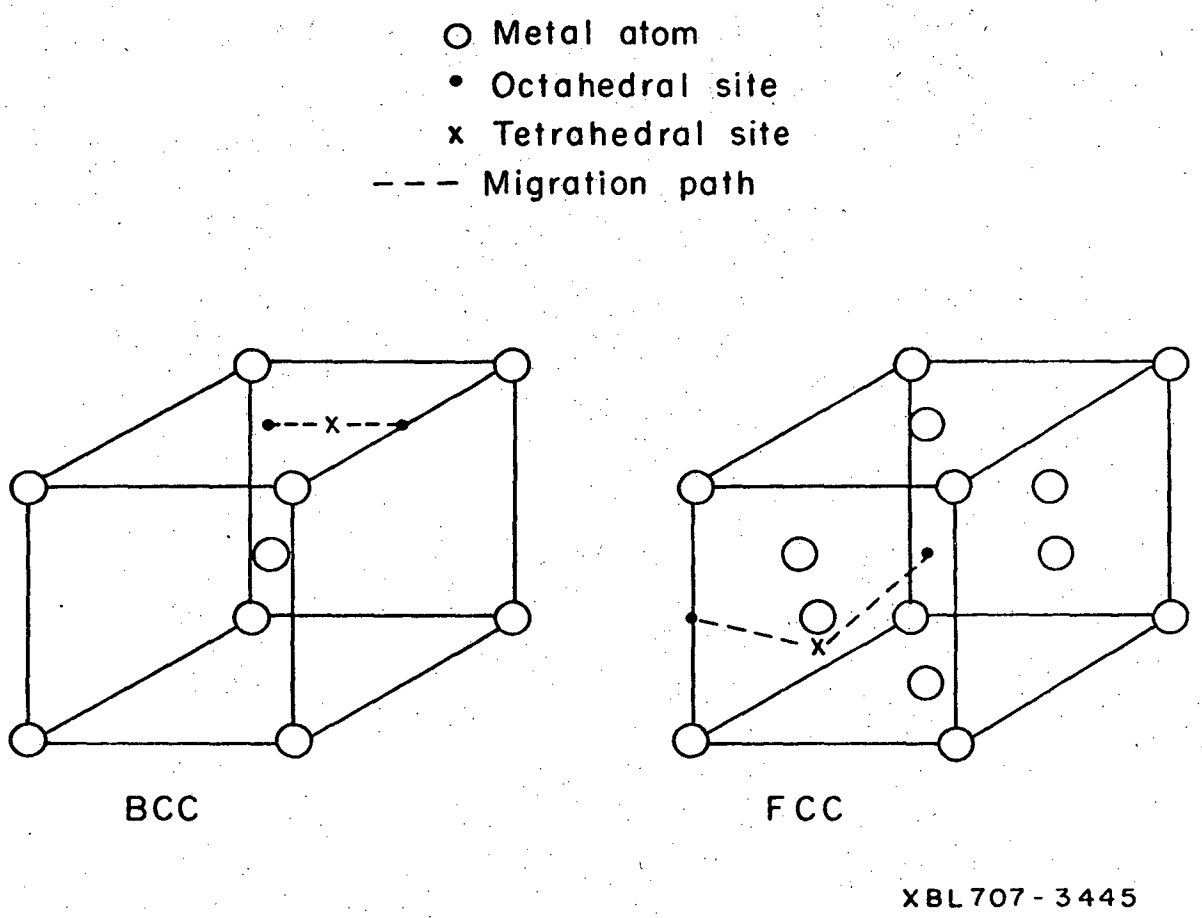
Metal atom
Octahedral site
x Tetrahedral site
Migration path
BCC
FCC
XBL707-3445

Fig. 1.

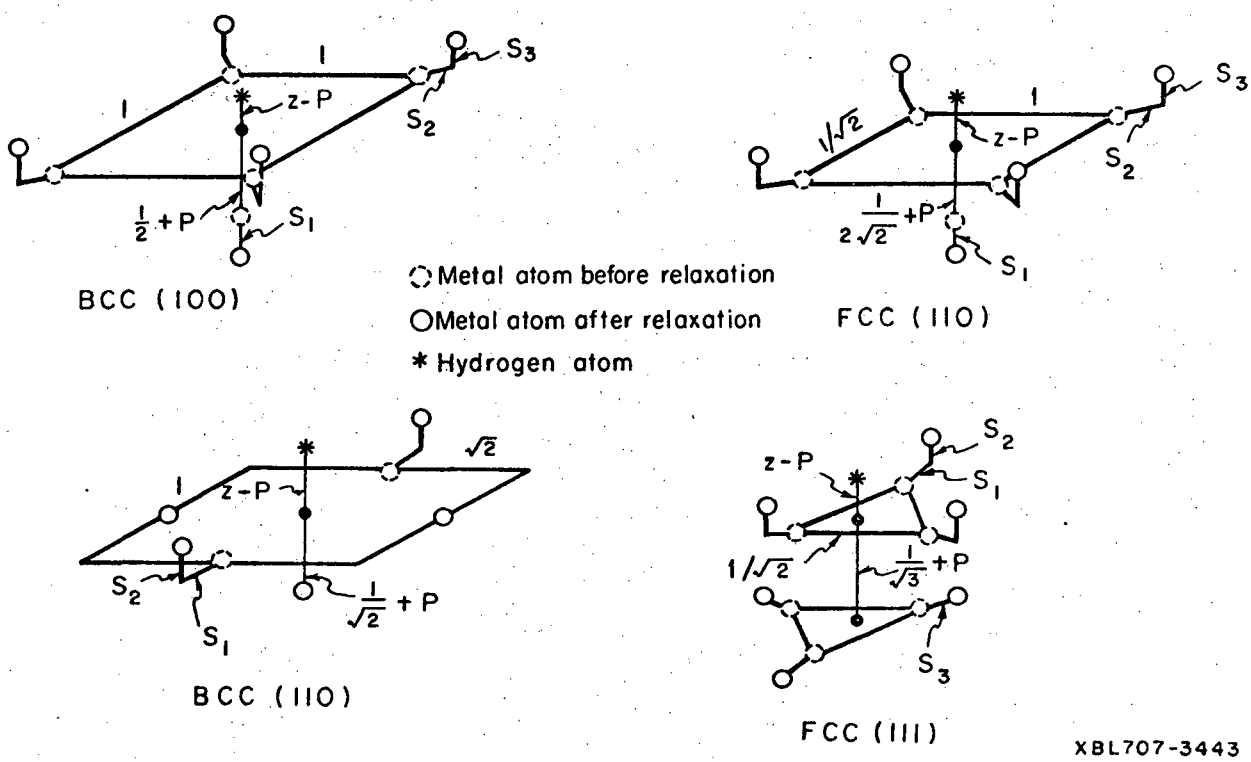
1
1
z-P
S3
S2
1/2 + P
S1
BCC (100)
Metal atom before relaxation
Metal atom after relaxation
* Hydrogen atom
1/√2
1
z-P
S3
S2
1/(2√2) + P
S1
FCC (110)
1
√2
z-P
S2
S1
1/√2 + P
BCC (110)
z-P
S2
S1
1/√2
1/√3 + P
S3
FCC (111)
XBL707-3443

Fig. 2

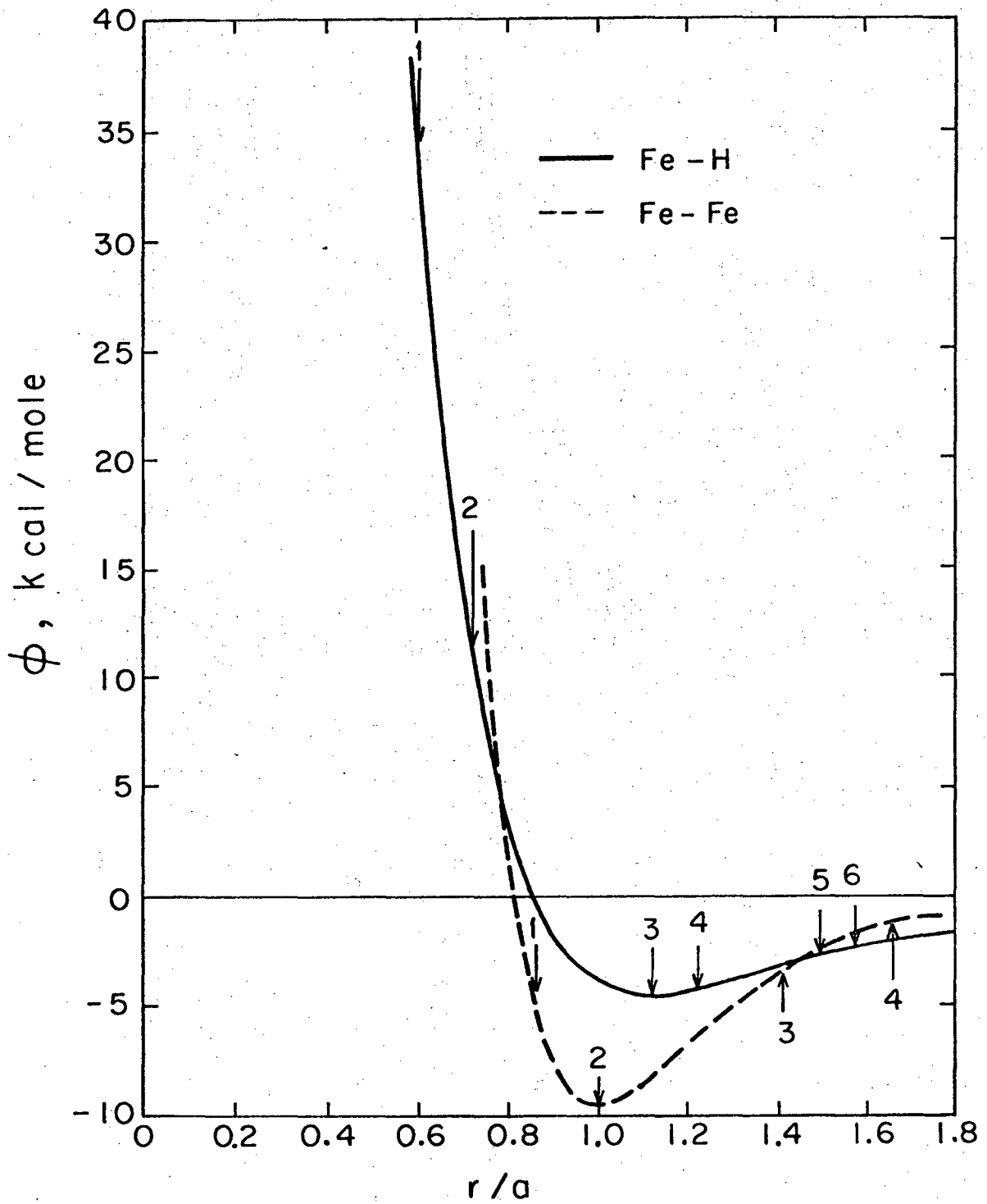


XBL707- 3444

Fig. 3

LEGAL NOTICE

*This report was prepared as an account of Government sponsored work. Neither the United States, nor the Commission, nor any person acting on behalf of the Commission:*

*A. Makes any warranty or representation, expressed or implied, with respect to the accuracy, completeness, or usefulness of the information contained in this report, or that the use of any information, apparatus, method, or process disclosed in this report may not infringe privately owned rights; or*

*B. Assumes any liabilities with respect to the use of, or for damages resulting from the use of any information, apparatus, method, or process disclosed in this report.*

*As used in the above, "person acting on behalf of the Commission" includes any employee or contractor of the Commission, or employee of such contractor, to the extent that such employee or contractor of the Commission, or employee of such contractor prepares, disseminates, or provides access to, any information pursuant to his employment or contract with the Commission, or his employment with such contractor.*

*TECHNICAL INFORMATION DIVISION*
*LAWRENCE RADIATION LABORATORY*
*UNIVERSITY OF CALIFORNIA*
*BERKELEY, CALIFORNIA 94720*